Research Square

Preprints are preliminary reports that have not undergone peer review.
They should not be considered conclusive, used to inform clinical practice,
or referenced by the media as validated information.

Optimisation of ZERON 100X solid wire for welding super duplex stainless steels to further improve weld pitting corrosion resistance

Glenn Byrne
NeoNickel Blackburn Ltd, UK
Zhuyao ZHANG
zzhang@lincolnelectric.eu

Lincoln Electric Europe https://orcid.org/0000-0001-7568-2649

Research Article

Keywords: Super duplex stainless steels, ZERON 100X, Welding, GTAW, GMAW, Pitting Resistance Equivalent Number (PREN), Pitting corrosion, ASTM G48A, ASTM A923C

Posted Date: October 28th, 2026

DOI: https://doi.org/10.21203/rs.3.rs-11241669/v1

License: This work is licensed under a Creative Commons Attribution 4.0 International License.
Read Full License

Optimisation of ZERON 100X solid wire for welding super duplex stainless steels to further improve weld pitting corrosion resistance

Glenn Byrne[1,a] and Zhuyao Zhang[2,b]

[1]NeoNickel Blackburn Ltd, Blackburn, UK

[2] Lincoln Electric Europe, Sheffield, UK (Corresponding author)

[a]e-mail: glenn.byrne1@outlook.com, [b]e-mail: zzhang@lincolnelectric.eu

Abstract

This paper presents the work conducted in optimizing the design of ZERON 100X solid wire for welding super duplex stainless steels (SDSS) to further improve the pitting corrosion resistance of the welds and meet the increased industrial requirements. The chemical composition of the modified wire has a substantially higher guaranteed Pitting Resistance Equivalent Number (PREN) while remaining within the limits specified for the classifications of ER2594 in AWS A5.9 and 25 9 4 N L in ISO 14343, thereby retaining compliance with relevant welding consumable specifications and pre-existing welding procedure qualifications. AWS-type all-weld metal assemblies, thin-wall pipe joints, thick plate joints, and all-weld deposit blocks were used to evaluate the new ZERON 100X filler wires. The microstructure, phase stability, mechanical properties, and corrosion resistance of the Gas Tungsten Arc Welding (GTAW) and Gas Metal Arc Welding (GMAW) welds and welded joints were assessed primarily in the as-welded condition. Selected GMAW joints were also tested in the post-weld solution annealed and water-quenched condition. Pitting corrosion performances in ferric chloride solutions were assessed in accordance with ASTM G48 Method A (ASTM G48A) and ASTM A923 Metod C (ASTM A923C). Critical Pitting Temperatures (CPT) were determined in simulated seawater solutions at potentials representative of chlorinated seawater (used in cooling water, fire protection and utility water systems on offshore oil and gas production) and high-pressure seawater feed in Sea Water Reverse Osmosis (SWRO) applications. The results are compared with those obtained using the conventional ZERON 100X consumables.

Keywords: Super duplex stainless steels, ZERON 100X, Welding, GTAW, GMAW, Pitting Resistance Equivalent Number (PREN), Pitting corrosion, ASTM G48A, ASTM A923C.

1 Introduction

The oil and gas industry has been continuously pursuing higher operating efficiency and design optimization of processing facilities [1]. This has led to progressively more demanding performance requirements for duplex and super duplex stainless steels and their welded joints, consequently imposing more stringent requirements on welding consumables. Historically, engineering practices specified a minimum PREN [2], [3] of 40 for cast and wrought SDSS based on the established correlations between increased PREN and enhanced resistance to pitting and crevice corrosions in chloride environments, including seawater [4], [5].

The PREN is defined as: PREN=%Cr+3.3%Mo+16%N and, where tungsten is present, PREN=%Cr+3.3(%Mo+0.5%W)+16%N.

Welding consumables for SDSS were originally developed to produce weld metals with an appropriate chemical composition capable of achieving the required austenite-ferrite phase balance while providing adequate strength, toughness, and corrosion resistance in both as-welded [6], [7] and post-weld heat-treated conditions [8]. Traditionally, to satisfy the corrosion properties expected of weld joints while maintaining the challenges to manufacturing process at a reasonable level, the super duplex welding consumables were designed to guarantee a minimum PREN of 40, with a

typical range of 40 to 42. This approach has successfully met the needs of industrial applications for many decades. However, issues continue to arise when facing even higher demands for corrosion performance.

Initially Shell argued that a PREN of 42.5 minimum was required for umbilical applications in the Gulf of Mexico [9]. This involved single pass welding of square edge butt welds in 1.65mm thick tubes. This is very different to welding thicker joints that require more weld passes. In 2011, ASTM A240 [10] was revised to require a minimum PREN of 42 for common wrought grades of SDSS (e.g. UNS S32760 and S32750). Subsequently, project specifications issued by various oil companies began requiring welding consumables to also meet PREN ≥ 42, together with testing at higher temperatures under ASTM G48A [11]. This is despite the Norwegian experience of fabricators struggling to meet G48A corrosion test requirements at 40 ℃ and subsequently reducing the test temperature to 35 ℃, without impact on operational performances [12].

However, in parallel, and without recognition of the Norwegian experience, there has been a growing trend for welded joints to meet ASTM A923C test requirements [13] [14]. This standard [15] uses ferric chloride solution, specifies a test temperature of 40°C for super duplex base metals and a maximum acceptable corrosion rate calculated from a corrosion rate of 10 mdd (approximately equivalent to 1 g/m^2 weight loss) for a 24-hour test duration. By comparison, the common acceptance level for weight loss when testing to ASTM G48A is 4 g/m^2 [16]. Further, ASTM A923C procedure and acceptance level for SDSS were developed on the performance of base plates and not weld metal or welded joint [17]. As far as the authors are aware, there has never been a technical justification of the application of ASTM A923C to welded joints in the way that the TWI verified ASTM G48A for welded joints [16]. This has resulted in difficulties in qualifying welding procedures to ASTM A923C when using consumables with PREN ≥ 40 (even when augmented with Argon (Ar) /Nitrogen (N_2) shielding gas) that have been highlighted in the literature [13], [14] and some of the limitations of this have been pointed out [18]. To overcome the issue, for some increasingly critical applications, users have selected over-alloyed hyper duplex consumables for welding SDSS to provide enhanced corrosion resistance in specific weld regions, particularly the root pass. In engineering practice, however, the use of these substantially over-matching composition filler metals presents significantly higher challenges in consumable manufacturing, weld fabrication and the metallurgical control of weld metal.

Consequently, welding consumable manufacturers have been required to supply filler metals for SDSS that match or exceed the PREN of the corresponding wrought products (i.e. PREN ≥ 42), and pass pitting corrosion tests under higher temperatures or to more stringent standards. At the same time, these filler metals still must satisfy the requirements for strength, low temperature toughness and weldability across a range of welding processes and joint thicknesses. All these demanding and often competing requirements underscored the need for the present work.

2 Composition adjustment

2.1 Computational thermodynamics and empirical predictions of phase balance

Computational thermodynamics is a discipline that uses thermodynamic theory combined with numerical methods and computer calculations to predict and analyse the stability, phase equilibria, and thermodynamic properties of multi component metallic systems. JMatPro® is a simulation software package that is capable of doing this work [19]. In the current study, a nominal composition that met the PREN 42 minimum with a typical range of 43 to 44 together with modifications to the additions of some other elements was selected and used the simulation software in an iterative way to establish a composition that also met the phase balance requirement of the weld metal.

To clearly distinguish the materials evaluated in the current work, the wire products are identified as ZERON 100X(A) and ZERON X(B), respectively corresponding to the original design specification (i.e.

A) and the new modified composition (i.e. B). The standard designation of the wire remains ZERON 100X. Table 1 shows the composition limits specified by the classifications ER2594 in AWS A5.9 [20] and 25 9 4 N L in ISO 14343-A [21], typical composition of the original ZERON 100X grade (i.e. ZERON 100X(A)) and the optimised composition ZERON 100X(B).

Table 1. Specification limits of AWS A5.9: ER2594 and ISO 14343-A: 25 9 4 N L, and typical compositions of the original wire Zeron 100X(A) and the optimised wire ZERON 100X(B)

Description	Wt%	C	Mn	Si	Cr	Ni	Mo	Cu	W	N	FN WRC-92	PREN[a]
ER2594 / 25 9 4 N L	Classification limits[b]	0.03	2.5	1.0	24.0-27.0	8.0-10.5	2.5-4.5	1.5	1.0	0.20-0.30	NS[c]	NS[c]
ZERON 100X(A)	Typical	0.015	0.70	0.25	25.0	9.2	3.60	0.60	0.60	0.22	55	41.4
	Heat example	0.016	0.64	0.21	25.4	9.1	3.57	0.57	0.64	0.22	59	41.6
ZERON 100X(B)	Typical	0.015	0.70	0.35	26.0	9.3	3.80	0.60	0.60	0.22	62	43.2
	Heat example	0.014	0.62	0.30	26.0	9.0	3.90	0.58	0.59	0.22	69	43.4

a. PREN = %Cr+3.3(%Mo+0.5%W)+16%N; b. Single values = maximum; c. NS = not specified.

From manufacturing consideration, the JMatPro® software was also able to predict an equilibrium phase fraction diagram that, at a solution heat treatment temperature of 1120 °C, the modified composition should provide the wire rod with a phase balance of approximately 44% ferrite and 56% austenite while avoiding the precipitation of deleterious phases that could seriously compromise drawability of the material, as indicated by the dotted line in Figure1.

According to WRC-1992 diagram [22], the estimated ferrite content in the microstructure from the new ZERON 100 X(B) composition is typically in the range of 60 to 70 FN which corresponds to a percentage range of approximately 40% to 60%. These compare with the original ZERON 100X(A) composition's 50 – 60 FN and 35% to 55% ferrite (Figure 2).

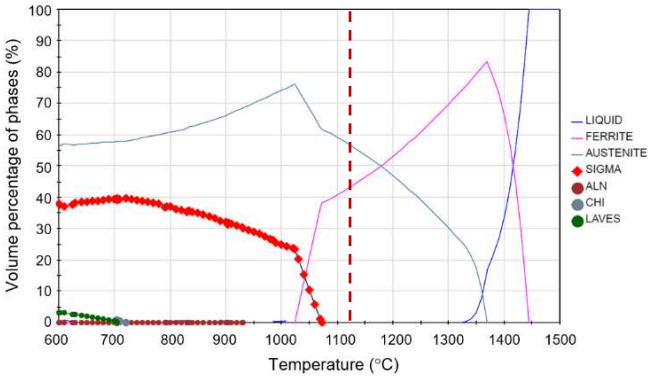


Figure 1. Predicted equilibrium phase fraction of Zeron 100X(B) composition

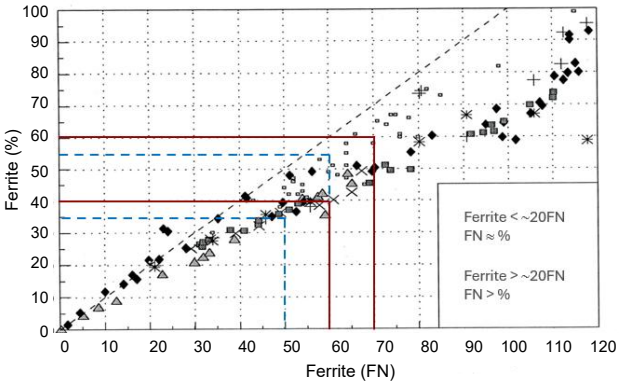


Figure 2. The expected ferrite content ranges from the ZERON 100X compositions [23]

2.2 Computational thermodynamics and empirical predictions of phase stability

The simulation software also provides the capability to predict Time Temperature Precipitation (TTP) curves for each of the nominal compositions. Figure 3 compares the predicted precipitation behaviours of the welds from ZERON 100X(A) with a PREN of 40.5, ZERON 100X(B) with a PREN of 43.3 and a generic 2509 type wire with a PREN of 43.1 [24].

The main difference in composition between ZERON 100 and 2509 is the additions of copper (Cu) and tungsten (W) between 0.5% and 1% in the ZERON 100 formulations. It has been argued that these elements promote the early precipitation of chi phase compared with 2509 [25] which has no deliberate additions of these elements. This seems counter intuitive as the diffusivity of W is an order of magnitude slower than that of molybdenum (Mo) and two orders of magnitude slower than

chromium (Cr) at 1000 °C. This would suggest slower precipitation characteristics. Indeed, the TWI carried out both long-term and short-term corrosion tests covering industrial environments and standard quality control corrosion tests and found no difference in performance between welded joints made with ZERON 100X (PREN 40.56) and with 2509 (PREN 41.22) when welded using low heat inputs ("well within typical industrial practice"), medium heat inputs ("at the top end of typical industrial practice"), and high heat input ("higher than typical industrial practice") [26]. This shows that the differences in precipitation characteristics between the two grades are of no practical significance.

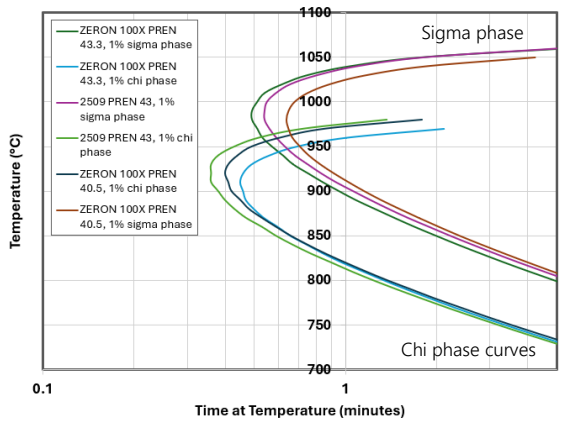


Figure 3. Predicted weld TTP curves for precipitation of 1% sigma phase and 1% chi phase in each of the alloys.

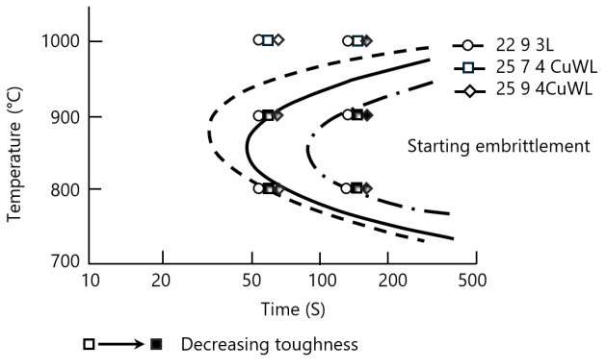


Figure 4. TTP curves of duplex and super duplex welds including one from a ZERON 100X(A) weld (typical PREN 40.5) based on loss of toughness [27]

As expected, the time to precipitate 1% sigma phase increases as the PREN of the consumable decreases. The sigma phase precipitation characteristics are very similar to other higher PREN material that does not contain copper and tungsten. The sigma "C" curve of the 2509 (PREN 43.1) falls between the ZERON 100X(B) (PREN 43.3) and the ZERON 100X(A) (PREN 40.5) "C" curves. Van Nassau et al [27] derived a TTP curve for conventional ZERON 100X(A) weld metal (25 9 4CuWL) with a nominal PREN 40.5 based on loss of toughness (Figure 4).

Table 2 details the TTP curves with respect to temperature and time for 1% precipitations of both sigma and chi phases. The predicted noses of the TTP curves for sigma phase for ZERON 100X(B) and the 2509 compositions both corresponded to a temperature of 985℃ and a time to first precipitate of about 29 and 27 seconds respectively, indicating little difference in the characteristics of sigma phase precipitation between the two compositions.

As expected, the lower PREN, ZERON 100X(A) composition takes longer to form the first precipitate, about 38 seconds, at a slightly lower temperature of 980℃. The time to precipitate corresponds well with the empirical work of Van Nassau [27] (about 30 seconds). However, the simulation predicts that the nose of the "C" curve is found at 980 ℃, while the empirical approach shows it to be at 890℃. This overestimate of the temperature for first precipitation has been observed by others when using this software package [24] and they attribute this to the software not properly accounting for the segregation effects found in real welds.

With respect to chi phase, the package predicts the temperature corresponding with the nose of the TTP curves for each composition varies by 10 °C. But the predicted time to precipitate, for the 2509 composition is faster (i.e. in 20 seconds) than that of the ZERON 100X(B) composition (i.e. precipitates in 27 seconds) with a very similar PREN level (a difference of 0.2). This finding contradicts other work [25] that claims that the opposite is the case.

Table 2. Locations of the noses of the TTP curves with respect to temperature and time for sigma and chi phases

Grade and differences	PREN	1% sigma phase precipitation		1% chi phase precipitation	
		Temperature (°C)	Time (S)	Temperature (°C)	Time (S)
Zeron 100X(A)	40.5	~ 980	~ 38	~ 923	~ 24
Zeron 100X(B)	43.3	~ 985	~ 29	~ 915	~ 27
Difference	+2.8	+5	-8	-8	+3
2509	43.1	~ 985	~ 32	~ 925	~ 20
Difference	+0.2	0	-3	-10	+7
Precipitation estimation (based on loss of toughness in Figure 4, Van Nassau [25])					
Zeron 100X(A)	40.5	Temperature = ~ 890 °C		Time = ~ 30s	

This part of the work indicates that the ZERON 100X(B) composition is unlikely to exhibit any drawability issues associated deleterious phases in the wire. It also suggests that its precipitation behaviour is very similar to 2509 composition already in use. This provided the confidence for advancing the commercial production of filler wires based on the optimised ZERON 100X(B) composition.

3 Production of the wires

The steel was produced using the Argon Oxygen Decarburization (AOD) steelmaking process, continuously cast into billets, rolled to 5.5 mm diameter rod coils, solution annealed, and acid pickled. The rod was then drawn to various finished product diameters, with processing parameters adjusted to suit the characteristics of the wire rod from the new composition. In the current work, 1.6 mm and 2.4 mm diameter cut-length GTAW rods, and 1.0 mm and 1.2 mm diameter spooled GMAW wires were produced. The drawability of the wire rod was satisfactory and yield losses were at the similar level as the original ZERON 100X(A) composition. The specified wire mechanical properties, microstructure, dimensional tolerance, ovality, straightness, helix, surface smoothness and cleanliness requirements were all met.

4 All-weld metal tests

4.1 All-weld metal tensile, Charpy impact and hardness tests

For all-weld mechanical property tests of the ZERON 100X(B) composition, the GTAW assembly was prepared using a diameter 2.4 mm rod with shielding gas of pure Ar, and the P-GMAW assembly was prepared using a wire of diameter 1.2 mm with newly designed synergic waveform and BOC Cronigon He30C (69.75%Ar+30%He+0.25%CO_2) mix gas. The tests were conducted in as-welded condition. The results are listed in Table 3.

Comparing with the properties of the original composition design, all-weld metals from the new composition wires showed identical level of tensile strength and elongation with slightly higher proof stress for both GTAW and P-GMAW. In the case of impact toughness, the GTAW welds are similar, but GMAW weld produced significantly higher values than historical data. This is considered owing to the positive effect by the P-GMAW waveform and the newly formulated shielding gas, which were developed primarily for improving the weld porosity resistance. Hardness saw an approximately 5 to 10 HV10 increase, but still well below the typical maximum limit level.

4.2 All-weld metal pitting corrosion tests

ASTM G48A and ASTM A923C tests were conducted to the all-weld deposit in as-welded condition. The deposit blocks were prepared using GTAW process with pure Ar shielding. The composition of the test blocks was analysed using Optical Emission Spectroscopy (OES) and ferrite measured with Fisher Ferritscope. The results are listed in Table 4.

Table 3. Results of GTAW and P-GMAW all-weld metal mechanical properties of ZERON 100X(B)

Processes	Tensile test at 20°C	Charpy impact test at -50 °C	Hardness test (HV10)

	Rp0.2 (MPa)	Rm (Mpa)	A4 (%)	A5 (%)	Absorbed energy (J) Average / individual	Mid-section Average / individual
AWS A5.9/ISO 3581 "expected minimum"	550	760	15	18	-	-
GTAW	720	872	28	26	133 / 126, 302, 137	299 / 294, 302, 302
P-GMAW	714	864	28	26	119 / 126, 120, 112	312 / 309, 309, 319

Table 4. Chemical composition and ferrite content of the deposit blocks for G48A and A923C tests

ID	C	Mn	Si	Cr	Ni	Mo	Cu	W	N[a]	PREN	Measured ferrite[b] (%)
GTAW rod	0.014	0.6	0.29	26.0	9.0	3.90	0.58	0.59	0.22	43.4	-
Block A (G48A)	0.015	0.6	0.32	26.0	8.6	3.81	0.54	0.55	0.18	42.4	60
Block B (A923C)	0.014	0.6	0.32	26.0	8.6	3.83	0.54	0.56	0.18	42.4	66

a. Nitrogen content of wire analysis was from Leco. The N content variation between wire rod and deposits are considered due to the analytical difference between Leco and OES, and small amount of loss through the GTAW arc.
b. Average of measurements from six areas across the top surface of each block.

To explore the potential effect of different test specimen surface conditions and the sensitivities of the modified composition to such influences, the specimens were prepared differently for comparison. For G48A, the surfaces of two specimens were polished to 120-grit finish as suggested in G48, but one tested without pickling (as specified by G48A) and the other after pickling. In the case of A923C, two surface finishes, 120-grit (the minimum specified by A923C) and 1200-grit (as recommended by TWI for duplex steel weldments [26]), were evaluated. The test temperature was 40°C and the exposure duration was set for 24 hours. The results are listed in Table 5.

Table 5. Results of ASTM G48A and ASTM A923C tests of ZERON 100X(B) GTAW all-weld metal

Test	Surface condition		Test temp. (°C)	Test duration (h)	G48A Weight loss (g/m^2)	A923C Corrosion rate (mdd)	G48A Pits X20 mag.
	Polish finish	Pickling					
ASTM G48A	120-grit	No	40	24	0.09	/	No
	120-grit	Yes	40	24	0.06	/	No
ASTM A923C	1200-grit	No	40	24	(equiv. 0.00)	0.00	/
	120-grit	No	40	24	(equiv. 0.329)	3.29	/

The weld deposits demonstrated significantly higher resistance to ferric chloride pitting attacks than the weld from original composition wire, i.e. ZERON 100X(A). All specimens passed G48A and A923C at 40 °C and demonstrated significant margines to satisfactorily meet the design expectations and the requirements of relevant standards. Pickling and 1200-grit surface finish showed certain extra help over non-pickling or 120-grit finish, but the degree of the observed effects was very marginal. The is considered an indication of robust corrosion resistance of the material with this level of PREN at the tested temperature. The results agree with the trend reported in an earlier investigation using SMAW deposits, where deposits with identical values of PREN, 43.88 and 43.72, achieved CTPs of 40.0 °C and 42.5 °C from ASTM G48 Method E test using specimens polished to 1200-grit finish [28]. It is considered reasonable to expect that the GTAW weld from the new ZERON 100X(B) consumable and 1200-grit finish should have the capability of achieving G48E CPT 42.5 °C, or higher.

5 Weld joint tests and validations

Weld joint tests were conducted with butt joints of SDSS pipes and flat plates of ZERON 100 and 2507 grades. The GTAW and pulsed GMAW (P-GMAW) joints in 20 mm thick UNS S32760 plates were welded at BOC Gasses Welding Laboratories. The GTAW joints in UNS S32760 2" Sch. 40S pipes were produced at the Butting Fabrication shop. A P-GMAW joint in UNS S32750, 25 mm thick plate was welded and subsequently solution heat-treated at 1120 °C by Valen Fittings Limited.

5.1 Manual GTAW butt joints in 2″ Sch. 40S pipes

5.1.1 Welding details

Two manually welded GTAW joints were made in 2″ Sch. 40S ZERON 100 pipes. The butt joints had a single-V groove preparation with 30° bevel, 1 mm root face and 2.5 mm root gap. The joints were welded in the 5G uphill position with DCEN polarity, using 1.6 mm diameter rod. The joints were produced with one joint using pure Ar for both shielding and backing gases, and the other using Ar+2%N_2 as shielding gas and pure Ar as backing gas. The oxygen content of the backing gas was 50 ppm at the start of welding. The heat input of the root welds ranged between 1.3 and 1.5 kJ/mm and the capping passes was between 0.9 and 1 kJ/mm. The welding performance of the new composition rod was found very similar to that of the original. The appearances of the weld cap and root were as expected for this type of the SDSS joint (Figure 5).

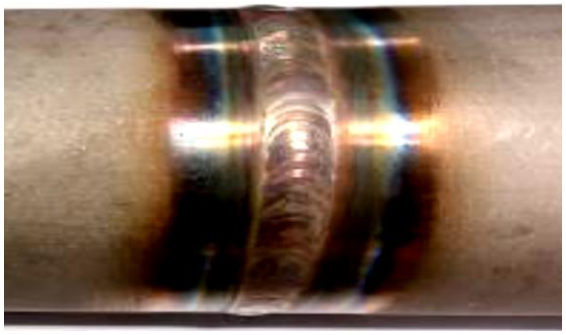
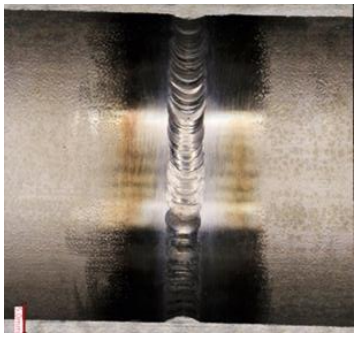
Cap pass  Root pass 

Figure 5. Surface appearances of the cap and root weld passes of the pipe joint

5.1.2 Metallurgical examination

A cross section of the weld joint produced with Ar+2%N_2 shielding and Ar backing was etched in 40% NaOH and examined under the optical microscope. The macro image of the cross weld joint and weld microstructure are shown in Figure 6. The microstructure observed consisted of typically distributed austenite and ferrite and was free from third phases. This was the cases in middle, cap and root of the weld and HAZ regions of the joint. Ferrite measurement was conducted in 9 locations around the weld as indicated in Figure 6. The ferrite content was ranged between 46% and 56% ferrite with an average of 49%.

5.1.3 Mechanical tests: tensile, Charpy impact and hardness tests

Cross-weld tensile, bend, and Charpy impact tests were conducted. The tensile test gave an UTS of 912 Mpa, and the 180° side bend test was satisfactory. The Charpy impact test was performed at -20 °C using sub-sized specimens with notches at the weld centreline. The results are listed in Tables 6 alongside equivalent values of full-size specimens converted using the conversion factor from ASTM A 370 Table 9.

Vickers hardness survey was carried out using 10 kg load. The locations of the indentations are shown in Figure 7 and the results in Table 7. The maximum hardness measured was 286 HV10 and from the cap area of the HAZ on both sides of the weld.

5.1.4 Corrosion tests

5.1.4a Corrosion tests in ferric chloride solutions.

The results of the ferric chloride testing are shown in Table 8. This includes results from testing to both ASTM G48A (TWI procedure [16]) and ASTM A 923C [15]. Table 8 also includes data from earlier work [29] on GTAW deposits of ZERON 100X(A) with PREN 40.72 using both Ar/Ar and Ar+2%N_2/Ar shielding/backing gas combinations. For the specimens used in the ASTM A923C test, the surfaces were all ground to 600-grit finish. In the case of the ASTM G48A specimens, only the cut edges were ground, and the test faces were kept in the as-welded condition.

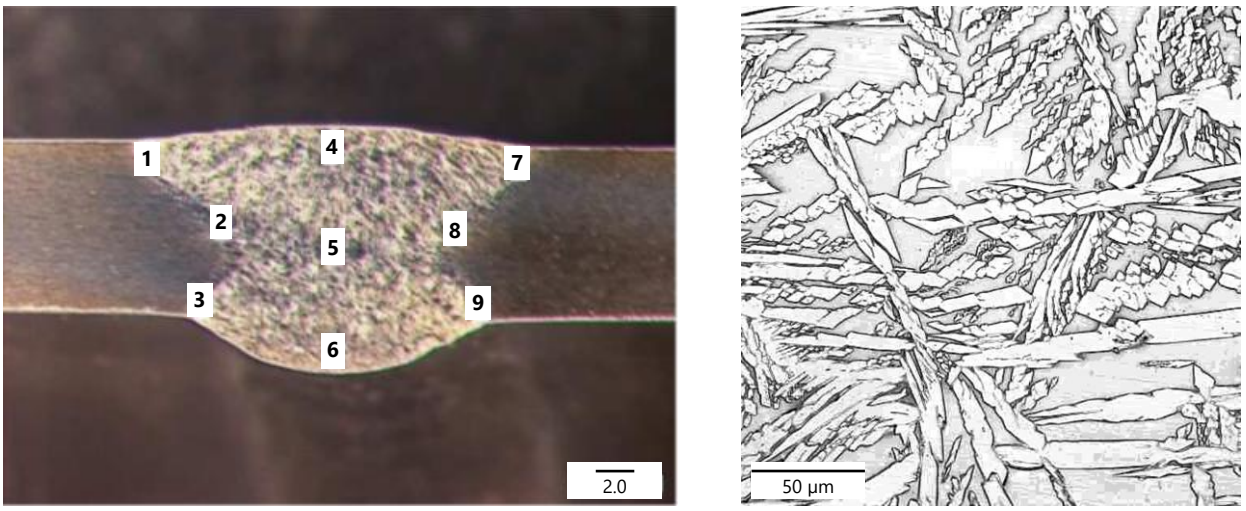


Figure 6. Microstructure of the 2″ Sch. 40S, Ar+2%N_2 / Ar weld joint using ZERON 100X(B) rod

Table 6. Results of Charpy impact test of the 2″ Sch. 40S pipe joint at -20°C (average of three values)

Specimen dimensions	Weld central line (J)	Fusion line (J)	Base metal (J)
Sub-sized CVN specimen (2.5x10x55 mm)	34.7	30.7	28.0
Converted to full size specimen (equv. 10x10x55 mm)	139	123	112

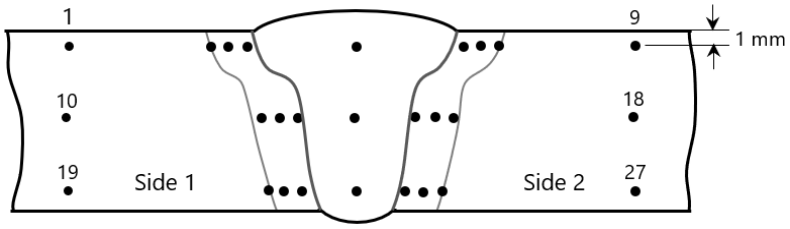


Figure 7. Illustration of hardness test indentation locations

Table 7. Results of the hardness survey (HV10) of the 2″ Sch. 40S pipe joint

Location	Base metal (side 1)	HAZ (side 1)	Weld metal	HAZ (side 2)	Base metal (side 2)
Cap	291	278, 282, 286	270	275, 275, 286	285
Middle	267	270, 280, 273	267	283, 276, 275	261
Root	281	272, 267, 274	271	278, 272, 270	275

The past data shows that welds produced using ZERON 100X(A) consumables with Ar/Ar shielding/backing gas readily passed G48A at 35 °C but struggle to pass at 40 °C. This is in line with the findings of Olsen [12]. Ar+2%N_2 shielding gas is often used to the test at 40 °C, but Gunn [30] and Metrode [31] indicated that the results with previous PREN 40 min consumables were variable. Results from the current work demonstrated that the welds made with the optimised composition, ZERON 100X(B) from both Ar/Ar and Ar+2%N_2/Ar gas combinations passed acceptance criteria of ASTM G48A at 40 and 45°C, and the ASTM A923C at 40 °C. These are in good agreement with the results achieved with all-weld deposit tests reported in Section 4.2.

5.1.5b. Potentiostatic electrochemical corrosion testing in simulated seawater

The electrochemical CPT test is more precise and differentiates more readily than testing in ferric chloride solutions. For this test, duplicate specimens were cut out from the 2″ Sch. 40S butt welds.

Table 8. Results of ASTM G48A and A923C tests on 2″ Sch. 40S pipe butt joints

Consumables	Shield./back. Gas combination	ASTM G48A (TWI procedure) (specimen condition: as-welded)	ASTM A923C at 40 °C (specimen condition: 600-grit finish)

		Test temp. (°C)	Weight loss (g/m^2)	Pits (x20 mag.)	Weight loss (g/m^2)	Corrosion rate (mdd)
ZERON 100X(A) PREN = 40.7	Ar / Ar	35	3.460	No	-	-
	Ar / Ar	40	< / >4	Yes/No	Poor performances	
	Ar+2%N_2 / Ar	40	0.217	No	Variable	
	Ar+2%N_2 / Ar	45	7.690	Yes	-	-
ZERON 100X(B) PREN = 43.0	Ar / Ar	40	0.592	No	0.088	0.88
	Ar / Ar	45	0.048	No	-	-
	Ar+2%N_2 / Ar	40	0.402	No	0.131	1.311
	Ar+2%N_2 / Ar	45	1.967	No	-	-
Acceptance criteria		4 g/m^2 max.; no pits			10 mdd (equiv.~1 g/m^2 weight loss) max	

The dimensions were 60 x 12 x 4 mm with the weld positioned across the centreline. The cut edges were ground to 240-grit, and the sharp edges were bevelled. All cut edges and the weld caps were acid pickled prior to testing to increase their corrosion resistance and to ensure that the corrosion resistance of the root pass was being measured as this is the surface that is exposed to the environment and is the most critical area of the joint. For electric connection, a 250 mm length of ZERON 100X(B) welding rod was tack-welded to one of the short edges. The tack weld and the lower portion of the rod were coated in lacquer to prevent wetting by the synthetic seawater. Electrochemical tests were carried out in 750 mL glass vessels filled with synthetic seawater prepared as follows, with the pH to 7.8-8.2 using NaOH.

NaCl-28g/L, $MgSO_4.9H_2O$ -7.74g/L, $MgCl_2.6H_2O$-6.02g/L, $CaCl_2.6H_2O$- 2.27g/L, $NaHCO_3$ -0.2g/L.

The test specimen was the working electrode. Graphite was used as the auxiliary electrode. A Standard Calomel Electrode (SCE) was the reference electrode. Compressed air was continuously bubbled through the synthetic seawater, and the specimens were mounted so that the water line was approximately 10 mm below the upper specimen edge to avoid crevice corrosion under the lacquer. This meant that the weld, both HAZ's and parent metal were completely immersed. The total surface area under water was approximately 13 cm^2. After sample immersion the potential was allowed to stabilize for about 15 minutes. The samples were then gradually polarised to the set potential of either +600 mV SCE or +200 mV over 30 minutes. The current was then allowed to stabilize for one hour at room temperature, after which the temperature was increased at a rate of 5 to 8 °C/h up to 90 °C, where it was held for two hours. A schematic of the test specimen and the experimental setup is shown in Figure 8.



Figure 8. Schematic illustration of the corrosion test specimen and the test set unit

The current density and temperature were monitored continuously throughout the test. Pitting was said to have initiated when the current density exceeded 10 $\mu A/cm^2$, if the passive current density at room temperature was less than 1 $\mu A/cm^2$. This follows the criteria set by Oldfield and Sutton [32]. After testing, the samples were washed, dried and examined under a microscope for indications of

corrosion. Figure 9 shows a typical plot of current density vs temperature and the appearance of the weld roots on completion of the test. The CPT results of the duplicate specimens were 52.5 ℃ and 56.3 ℃ at +600 mV SCE and 69.1 °C and 70.1 °C at +200 mV SCE for welds made using ZERON 100X(B) composition wires. These results will be compared with earlier work [29] done on ZERON 100X(A) consumables later.

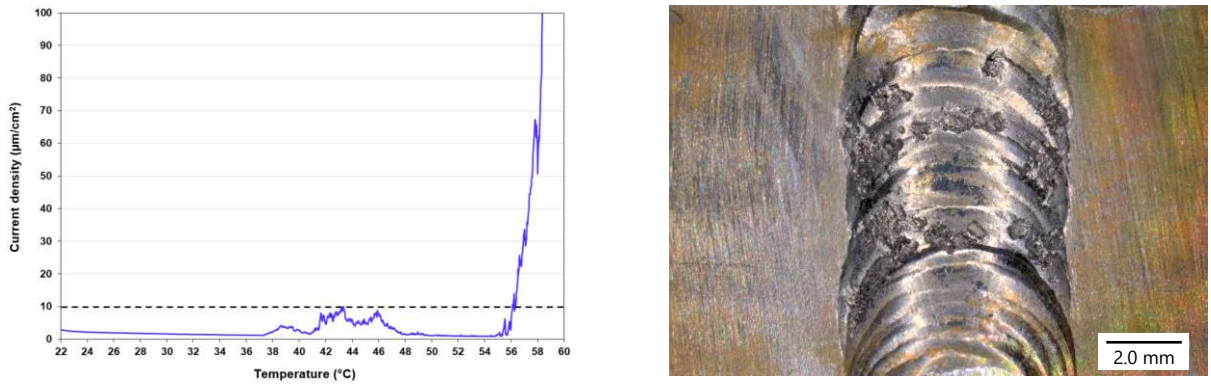


Figure 9. A typical plot of the current density changes with increasing temperature and a photograph of the root run of the weld on completion of the test showing the sites of pitting corrosion attack

5.2 Manual GTAW of 20mm thick ZERON 100 plate joint test

5.2.1 Welding details

GTAW weld joint of 20 mm thick plate was prepared to facilitate tests of the weld and cross joint properties in thick sections for comparison with lower PREN (i.e. 40 min) weld results. The joint preparation and weld pass sequence are illustrated in Figure 10 (a and b). Two weld joints were welded with 2.4 mm diameter GTAW rod, one using Ar for both shielding and backing gas, and the other used Ar+2%N_2 as shielding gas and Ar as backing gas. The first joint was used for all tests while the second joint was for metallurgical examination and corrosion test only. The oxygen content in the backing gas at the start of welding was 200 ppm. The heat input of the root pass was approximately 1.5 kJ/mm, with fill and cap passes ranging from 1.1 to 1.3 kJ/mm. The maximum inter-pass temperature was 100 °C. Radiographic inspection was performed in accordance with ISO 17636-1/ASME IX, using acceptance levels from ISO 5817/ ASME B31.3, and results were found to be satisfactory. The bend tests were also satisfactory.

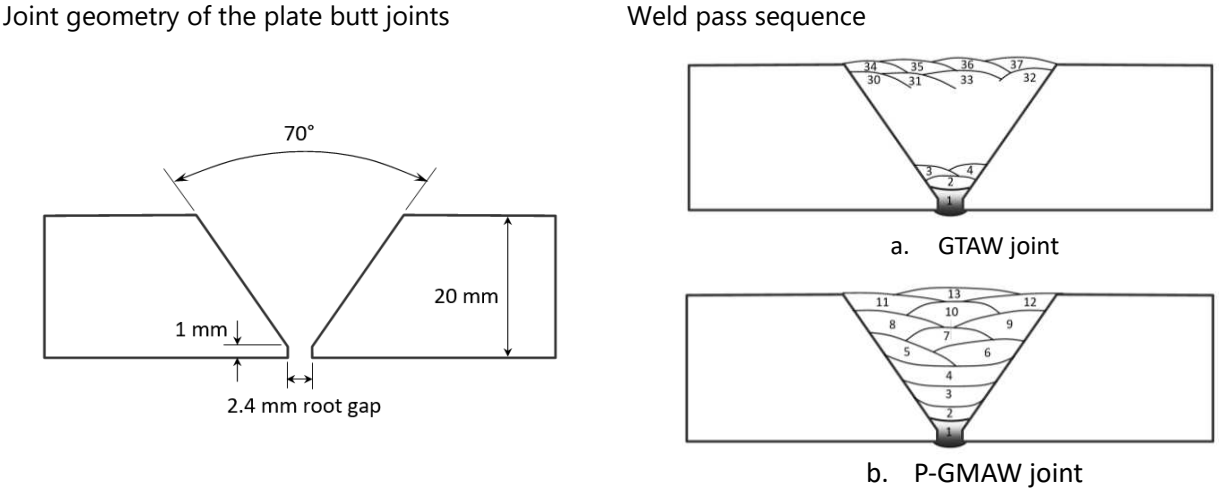


Figure 10. Illustration of joint geometry and run sequence of GTAW and P-GMAW butt welds

5.3.2 Metallurgical examination

Cross sections of the welds were etched in 40% NaOH. The microstructure imagines of the welds are shown in Figure 11. The microstructure of the joints was as expected as austenite-ferrite and free from third phases. The phase balance was measured using point counting to ASTM E562-19. A

magnification of x500 was used. Total field was 32 with 25 points per field. The results are presented in Table 9. The Ar+2%N_2 shielding gas tends to promote austenite formation in the weld deposit.

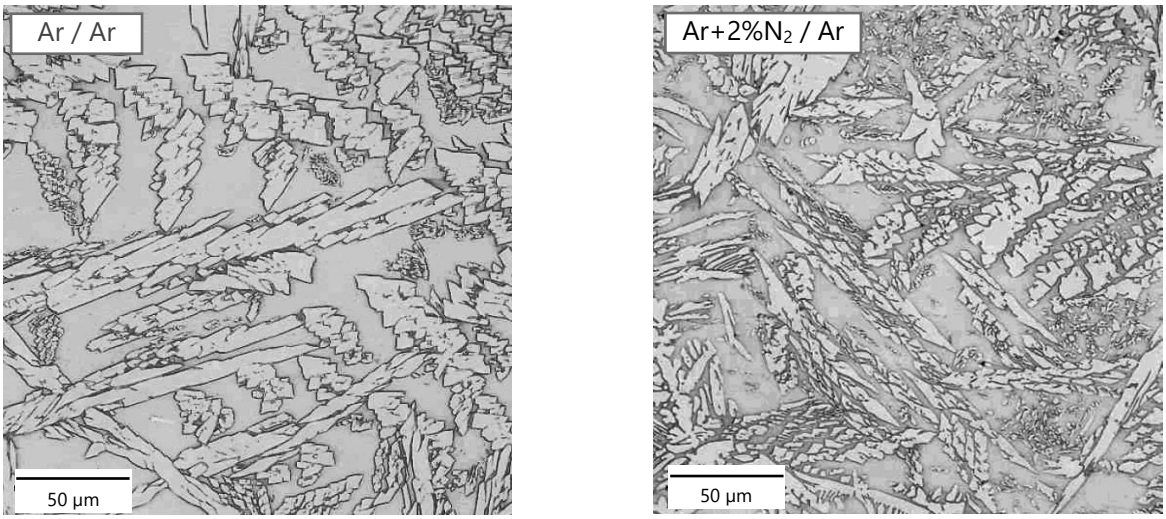


Figure 11. Microstructure of root weld of the 20 mm thick GTAW joint from ZERON 100X(B) rod

Table 9. Results. of ferrite content measurements[a]

Shield./back. gas combination	Ar / Ar				Ar+2%N_2 / Ar			
Field location	Volume fraction of δ-ferrite (%)	+/-95%CL	%RA	SD	Volume fraction of δ-ferrite (%)	+/-95%CL	%RA	SD
Weld metal cap	68.5	3.29	8.17	9.14	50.5	3.84	7.60	10.64
Weld metal root	45.4	3.04	6.40	3.04	45.4	2.77	6.21	7.68

a: Ferrite measurement from point counting conducted in accordance with ASTM E562-19.

5.2.3 Tensile, Charpy impact and hardness tests

The results of cross weld and all-weld tensile tests at ambient and elevated temperatures are shown in Table 10. All properties exceed acceptance levels. The results of Charpy impact test over a range of test temperatures are shown in Table 11. The Absorbed energy values show a high level of toughness and exceed the industry standard acceptance level of 50 J minimum at -46 °C.

Table 10. Results of all-weld metal and cross-weld tensile test at ambient and elevated temperatures

Temperature (°C)	25			100			200		
Tensile properties	Rp0.2 (MPa)	Rm (MPa)	A (%)	Rp0.2 (MPa)	Rm (MPa)	A (%)	Rp0.2 (MPa)	Rm (MPa	A (%)
Weld centre	734	915	26	688	833	24	606	755	27
Cross weld	-	799	-	-	707	-	-	679	-
Acceptance levels	550	750	15	470	700	/	430	670	/

Table 11. Results of Charpy impact test results at different temperatures (average of three values)

Test temperature (°C)	20	-25	-46	-50	-55	-70
Average impact energy (J)	128	147	134	123	115	103
Acceptance level	ISO 17781-QL1: average 50J minimum @-46 °C					

Vickers hardness HV10 surveys were carried out. The locations of the indentations are shown in Figure 12, and the results are shown in Table 12. The maximum hardness measured was 331 HV10 in the weld metal root.

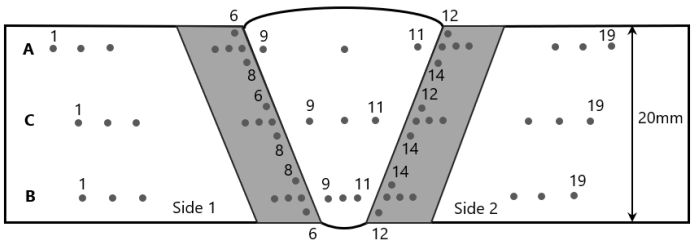


Figure 12. Locations of hardness indentations in the GTAW plate joint

Table 12. Results of the hardness survey (HV10) of the 20mm thick plate GTAW weld joint

Location	BM (side 1)	HAZ (side 1)	Weld centre	HAZ (side 2)	BM (side 2)
Cap (A1-A19)	260, 260, 266	272, 277, 269, 277, 271	289, 304, 292	277, 284, 284, 275, 278	280, 279, 277
Middle (C1-C19)	264, 270, 271	300, 297, 293, 298, 306	296, 303, 296	287, 298, 297, 292, 310	288, 278, 269
Root (B1-B19)	283, 275, 274	313, 322, 326, 310, 324	327, 331, 302	312, 313, 317, 319, 313	288, 286, 289

5.2.4 Corrosion tests in ferric chloride solutions

Welds from the 20 mm thick GTAW test plate welded with the ZERON 100X(B) composition wire were submitted to ASTM G48A test at temperatures of 40 °C and 45 °C, and to ASTM A923C test at 40 °C. The surface conditions of the tested specimens were as-welded for G48A and polished to 600-grit for A923C. The results of the tests are shown in Table 13. Welds made with the optimised consumable composition passed ASTM G48A at both 40 °C and 45 °C, and the ASTM A923C acceptance criteria.

Table 13. Results of ASTM G48A and A923C tests of the 20mm thick plate GTAW weld joint

Test method	Specimen surface condition	Test temperature (°C)	Ar / Ar		Ar+2%N_2 / Ar	
			Weight loss (g/m^2)	Pits	Weight loss (g/m^2)	Pits
ASTM G48A	As-welded	40	0.592	No	0.402	No
	As-welded	45	0.418	No	1.3976	No
	Acceptance level		4 g/m^2 max. and no pit (x20 mag.)			
ASTM A923C	600-grit	40	~ 0.088 (0.88 mdd)	No	~ 0.131 (1.31 mdd)	/
	Acceptance level		10 mdd (equivalent to ~1 g/m^2 weight loss)			

5.3 Automatic synergic P-GMAW of 20 mm thick test plates

5.3.1 Welding details.

A series of 20 mm thick test plates were welded using automatic synergic P-GMAW process. The weld preparation and run sequence are shown in Figure 10 (a and c). The root welds were made using 2.4 mm diameter GTAW rod using Ar+2.5%N_2 shielding and Ar backing gas combination. The filling and capping passes were produced with synergic P-GMAW using 1.2 mm diameter ZERON 100X(B) wire and Cronigon He30C shielding gas. The heat input of the root pass was between 1.13 and 1.77 kJ/mm, the fill and cap passes were run at about 1 kJ/mm. These weld joints were radiographically tested to ISO 17636-1/ASME IX, with acceptance levels to ISO 5817/ ASME B31.3, and results were found to be satisfactory. The results of bend test were also satisfactory.

5.3.2 Metallurgical examination

A cross section of the joint was etched in 40% NaOH. Metallurgical examination showed that the microstructure of the weld and HAZ consisted of austenite and ferrite, and they were free from intermetallic phases. The ferrite content was measured by point counting in accordance with ASTM E562-19 at a magnification of x500. The results, which comply with the requirement of ISO 17781, are presented in Table 14. Figure 13 shows an example of the weld microstructure.

5.3.3 Tensile, Charpy impact and hardness tests

The results of cross-weld and all-weld metal tensile tests at ambient and elevated temperatures of 100 °C and 200 °C are shown against specified minimum requirements in Table 15. All strength levels exceeded the minimum specified requirements by a significant margin.

The results of transverse Charpy impact tests over a range of test temperatures down to -70 °C for the different regions of the synergic P-GMAW joint, including the weld centre, fusion line and HAZ at fusion line +2 mm, are shown in Table 16. The results demonstrate a significantly excellent impact toughness, exceeding the industry standard acceptance level of 50 J minimum at -46 °C when tested at -50 °C.

Table 14. Ferrite content at different locations in the 20 mm thick plate P-GMAW weld joint

Location	Ferrite (%)	STD DEV	95% CL	% RA
Weld – cap	45.75	7.11	2.56	5.60
Weld – middle	47.38	6.9	2.49	5.26
Weld – root	44.75	8.41	3.03	6.77
HAZ – cap	63.38	6.27	2.26	3.57
HAZ – middle	64.75	10.58	3.81	5.88
HAZ – root	64.88	8.11	2.92	4.50
ISO 17781 requirement: 30% to 70%				

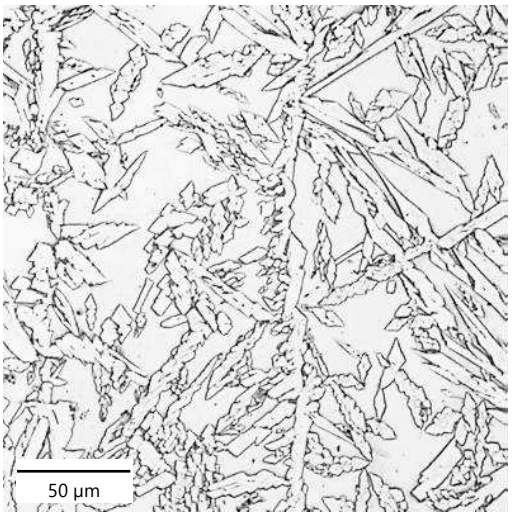


Figure 13. Microstructure of the weld root of the 20 mm thick plate weld joint produced with synergic P-GMAW using ZERON 100X(B) wire

Table15. Results of tensile test for the 20 mm thick plate P-GMAW butt weld joint

Test temperatures (°C)	Specified min. tensile strength		Weld centre		Cross-weld	
	Rp0.2 (MPa)	Rm (MPa)	Rp0.2 (MPa	Rm (MPa)	Rp0.2 (MPa)	Rm (MPa)
20	550	750	715	905	676	832
100	470	700	554	815	575	735
200	430	670	515	753	514	696

Vickers hardness HV10 surveys were carried out. The locations of the indentations are shown in Figure 14, and the results are shown in Table 17. The maximum hardness measured was 333 HV10. This result was from the weld metal root location.

Table 16. Results of Charpy impact test of the 20 mm thick plate P-GMAW weld joint

Test temperature (°C)	Weld centre, ave. (ind.) (J)	Fusion line, ave.(ind.) (J)	Fusion line + 2 mm, ave. (ind.) (J)
20	157 (151, 160, 160)	230 (231, 220, 238)	299 (302, 297, 297)
-20	154 (159, 156, 147)	-	-
-40	152 (149, 155, 152)	-	-
-50	130 (130, 126, 134)	138 (114, 149, 152)	185 (189, 158, 207)
-60	129 (122, 133, 131)	-	-
-70	120 (117, 120, 122)	-	-

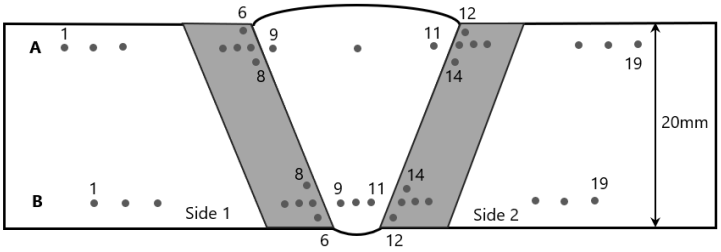


Figure 14. Locations of hardness indications in the weld joint of the synergic P-GMAW weld

Table 17. Results of the hardness survey (HV10) of the 20mm thick plate P-GMAW weld joint

Location	BM (side 1)	HAZ (side 1)	Weld centre	HAZ (side 2)	BM (side 2)
Row A	279, 281, 275	271, 279, 286, 295, 278	296, 287, 287	291, 288, 289, 276, 309	279, 281, 276
Row B	271, 260, 268	293, 312, 300, 299, 304	297, 311, 333	328, 301, 292, 291, 300,	256, 272, 266

5.3.4 Corrosion test in ferric chloride solutions

ASTM G48A test was conducted over a range of test temperatures, and ASTM A923C test was conducted at 40 °C. The GTAW root passes were machined out of the welds so that the assessment results would only reflect the performance of the P-GMAW weld metal. The results are shown in Table 18. Welds made with the optimised consumable composition passed the acceptance criteria of ASTM G48A at 35, 40, and 45 °C, and ASTM A923C at 40 °C.

Table 18. Results of ASTM G48A and A923C tests of the 20 mm thick plate P-GMAW weld joint

Sample surface condition	Test temperature (°C)	ASTM G48A		ASTM A932C
		Weight loss (g/m^2)	Pits (x 20 mag.)	Corrosion rate (mdd)
As welded	35	2.002	No	-
As welded	40	2.386	No	-
600-grit	40	-	-	3.36 mdd (~ 0.336 g/m^2)
As welded	45	2.092	No	-
As welded	50	108.820	No	-
Acceptance level		4 g/m2 max.	No pits	10 mdd (~ 1 g/m^2) max.

5.4 Weld joint of synergic P-GMAW 25mm thick UNS S32750 plate subjected to post weld solution heat treatment

5.4.1 Welding and heat treatment details

To test weld properties of ZERON 100X(B) after post weld solution heat treatment, a joint was produced using a 25 mm thick UNS S32750 base plate. The butt joint was a single-V groove preparation with 30° bevel, 1 mm root face and 2.5 mm root gap. The weld root was welded with GTAW using Ar/Ar shielding/backing gas combination. The fill and cap welds were produced using synergic P-GMAW with shielding gas 50%Ar+50%He (BOC Alushield Universal). The heat input was

1.3 kJ/mm and the inter-pass temperature was 100 °C maximum. The joint was completed in about 20 passes. The welded joint was solution heat treated at 1120 °C for 1.5 hours, then water quenched.

5.4.2 Metallurgical examination

A cross section of the weld was etched in a solution of 10% oxalic acid plus 40% NaOH, and then examined. The weld metal microstructures at the cap, mid-thickness, and root locations are shown in Figure 15.

The ferrite content in the weld metal cap, mid-thickness and root locations was measured by point counting in accordance with ASTM E562-19 at a magnification of x400. The results are shown in Table 19 and comply with the specification requirements. However, compared to the welds in the as-welded condition presented in the earlier sections, the microstructure exhibited a tendency toward slightly higher austenite due to the overmatching nickel content of the filler metal and the post-weld solution heat treatment.

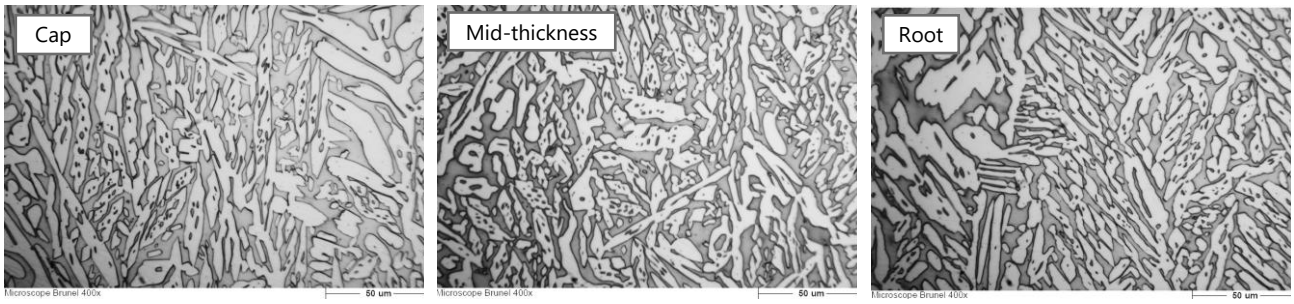


Figure 15. Microstructure of the manual synergic P-GMAW weld after post weld solution heat treatment

Table 19. Results of ferrite content measurement of the P-GMAW weld joint after solution heat treatment

Location	Ferrite (%)	STD DEV	95%CL	% RA
Weld – cap	34.1	1.77	5.21	5.56
Weld – middle	36.7	1.98	5.40	6.20
Weld – root	38.7	2.12	5.48	6.63
ISO 17781 requirement 30% to 70%				

5.4.3 Cross weld tensile test and Charpy impact test

The results of cross weld tensile test are shown in Table 20. The strength of ZERON 100X(B) welds exceed the specified minimum requirements across the range of test temperatures investigated.

Table 20. Results of cross-weld tensile test of the synergic P-GMAW weld joint after solution heat treatment

Test temperatures (°C)	Specified minimum tensile strength based on ZERON 100(A)		ZERON 100(B) weld after solution annealing and water quenching	
	Rp0.2 (MPa)	Rm (MPa)	Rp0.2 (MPa)	Rm (MPa)
20	550	750	629	827
100	470	700	575	741
200	430	670	514	683
250	400	650	488	709

Transverse Charpy impact tests were made with the V notch located at the weld metal centre line location. The results are shown in Table 21. The results obtained exceed industry standard toughness requirements.

5.4.4 Corrosion test in ferric chloride solutions

Corrosion tests were carried out to ASTM G48A at 40 °C and 45 °C with no pre-pickling to the specimens. The weight loss results were 0.0817 and 0.8743 g/m^2 respectively and no pits were observed.

Table 21. Results of Charpy impact test of the synergic P-GMAW weld joint after solution heat treatment

Location	Test temperature (°C)	CVN1 (J)	CVN2 (J)	CVN3 (J)	Average (J)
2 mm below cap surface	-50	154	122	127	134
Mid-thickness	-50	100	123	119	114
Acceptance level: ISO 17781-QL1, average 50J minimum @ -46 °C					

6 Benchmarking of the ZERON 100X(A) and ZERON 100X(B)

6.1 Microstructure and phase balance

Control of heat input, inter-pass temperature and welding technique has been necessary to avoid the problems of precipitation of third phases in joints of PREN 40 minimum filler metals [4]. The same controls were applied in the production of the test plate welds from the new ZERON 100X(B) filler wires. All the microstructures examined were free from intermetallic particles confirming the indications by the TTP curves predicted by the computational thermodynamics.
Given that no third phases were found in any of the microstructures of the welds, it is considered that the modified consumable alloy content and increased PREN from 40 minimum to 42 minimum (with typical range of 43 – 44) do not practically influence the microstructure quality or precipitation characteristics for the range of joint thicknesses and welding processes considered, provided best practice is applied.

Although not specifically discussed in the current work, these consumables are also often used for the repair welding of super duplex stainless-steel castings. Several end-users of pumps and valves in the desalination industry now specify a minimum PREN of 42 or higher for super duplex stainless-steel castings to achieve better corrosion resistance. ASTM A995 [33] mandates the post-weld solution heat treatment of major repairs in castings. For grade 5A super duplex castings, it specifies furnace cooling from 1120 °C to a temperature no lower than 1045 °C before quenching, while for grade 6A, the castings can be directly quenched from 1100 °C to ambient, or furnace cooled to 1050 °C and held for a minimum 15 minutes prior to quenching. However, Kotecki [34] exposed an unintentional consequence of this when using welding consumables with overmatching nickel content. The top of the TTP curve is slightly shifted to higher temperatures, meaning that furnace cooling to 1045 °C or 1050 °C can lead to sigma formation in the weld repairs. This effect is expected to be more pronounced for higher PREN weld metals (see Figure 3). Consequently, when using higher PREN consumables over-alloyed with nickel, furnace cooling to temperatures lower than 1100 °C should be avoided.

Phase balance is principally determined by the nickel and chromium equivalents of the consumable [21], and these are carefully controlled by the alloying design. The ferrite content of the 2" Sch. 40S pipe joints ranged between 46% to 56%. The ferrite content of the GTAW weld metal in the 20 mm thick plate joints ranged between 52.25% to 55.13%. The 20 mm thick synergic P-GMAW weld metal ranged between 44.37% and 64.88% ferrite. It is generally accepted that roughly equal proportions of austenite and ferrite in the weld is the optimum balance [35] and the results demonstrated this has been achieved. Indeed, the welds from the optimised filler wire readily meets the acceptance levels in ISO 17781 [36] of 30% to 70% for welds in the "as-welded" condition. It should be recognised that the significance of phase balance measurement has been called in to question [35], since it does not directly relate to either toughness or corrosion resistance and, it cannot be reliably measured to better than +/-6%. With respect to weld procedure qualification, it has been recommended that qualification be based on direct testing of toughness and corrosion resistance with phase balance measurement for information only.

6.2 Tensile properties

Figures 16 and 17 show the weld metal and cross-weld tensile properties achieved of the weld joint of ZERON 100X(B) at different temperatures and compared against the specified minimum requirements. All results exceeded the requirements across the range of temperatures investigated. When comparing with the typical values of the GTAW joint from ZERON 100X(A), the proof strength of ZERON 100X(B) weld was slightly higher, while the tensile strength of both weld and cross-weld was very similar.

6.3 Charpy impact toughness properties

Charpy impact transition curves detailing the results from the ZERON 100 X(B) 20 mm thick GTAW and synergic P-GMAW test plates and comparing it with data from ZERON 100X(B) welds of similar thickness is shown in Figure 18.

The impact toughness of the GTAW and P-GMAW welds are excellent and readily exceed specified minimum levels. However, the specified minimum levels were first published in 1991 [37] when there was relatively little experience with GMAW and the figures were probably set at conservative levels.

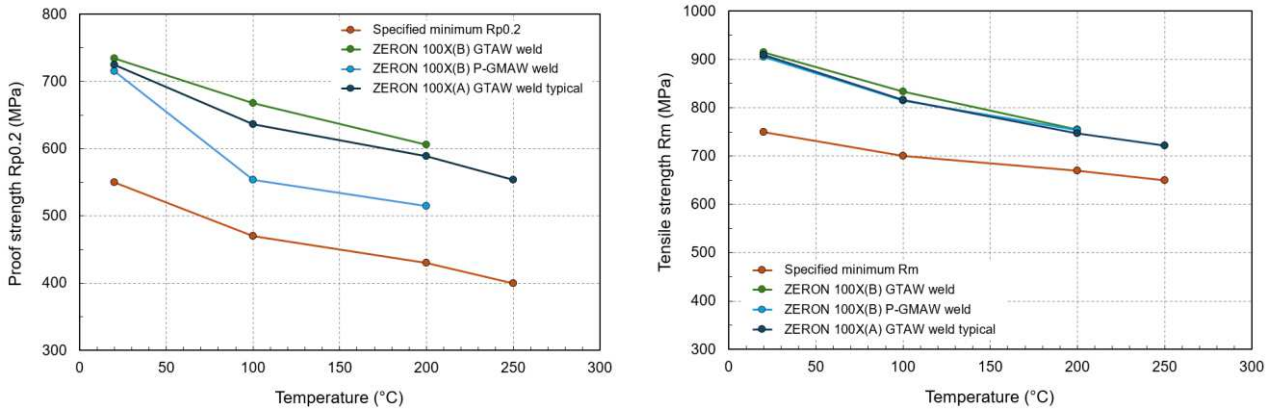


Figure 16. Weld Rp0.2 and Rm strength vs specified minimum

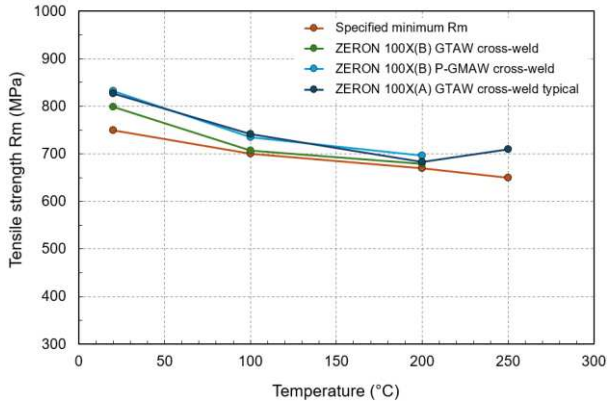


Figure 17. Cross-weld tensile strength of weld joints of ZERON 100X(A) and ZERON 100X(B) vs specified minimum requirements

The increased PREN appears to have no influence on the impact toughness properties as the results from the improved composition wire are very similar to toughness results reported in the literature [38] for PREN 40 welds of the same thickness. The toughness levels achieved support the metallurgical observation of freedom from intermetallic phases.

There appears to be little difference between the toughness of the synergistic P-GMAW and the GTAW weld metals. This contrasts with earlier studies concluding that GTAW weld toughness was significantly higher than that of GMAW [37]. At that time, data for GMAW was minimal, and the gas

mixtures (such as Ar+CO_2 and Ar+O_2) tended to lower toughness by forming a higher proportion of oxide inclusions in the weld metal. More recent gas formulations have evolved, providing better arc protection and enhancing penetration and metallurgical stability of the weld metal, thereby producing higher toughness [39].

6.4 Hardness properties

Table 22 shows the maximum Vickers hardness measured in each of the joints and the locations.

When NACE MR 0175 [40] transitioned to ISO 15156 [41] in 2003, references to grade specific hardness requirements were removed, subsequently NORSOK M-601 Edition 5 of April 2008 [42] and NORSOK MDS M630 Edition 5 of September 2010 [43] removed limits for maximum hardness for duplex stainless steels. Similarly, BS/EN 4515 [44] does not apply hardness limits for duplex pipelines. However, Section 7, Table 7-11 of DNV-OS-F101October 2010 [45], limits weld metal and HAZ hardness to 350 HV10. The GTAW and P-GMAW deposits made using ZERON 100X(B), the higher PREN filler wires, readily meets this requirement.

Table 22. A summary of the locations of the maximum hardness measured in each of the joints.

Joint	HAZ maximum hardness		Weld metal maximum hardness	
	Location	HV10 max.	Location	HV10 max.
2" Sch. 40S pipe GTAW joint	Cap	286	Root	271
20mm thick plate butt GTAW joint	Root	326	Root	331
20mm thick plate butt synergic P-GMAW	Root	328	Root	333

6.5 Corrosion resistance properties

6.5.1 Corrosion tests in ferric chloride solutions

GTAW and synergic P-GMAW welds made using ZERON 100X(B) consumables tested in the as-welded condition (without pretest acid pickling) passed ASTM G48A test at 45 °C. They also passed ASTM A923C at 40 °C. This is a significant step forward as welds made using ZERON 100X(A) type consumables required alloying with nitrogen through the shielding gas, to meet G48A test requirements at 40 °C [4]. Even with such measures, the passing rate has been moderate and sensitive to the small variables randomly introduced during the welding process. Furthermore, experience with passing ASTM A923C when using the ZERON 100X(A) consumable, even when augmented with Ar+N_2 shielding gas, has been tortuous. The applicability of this test to welded joints has been called in to question [13],[14]. Nevertheless, the use of the ZERON 100X(B) consumable does provide a solution to the challenges of this test provided the welded sample is ground to 600-grit all over to remove any scale or surface contaminants that could contribute to weight loss during the test. This is acceptable method of test specimen preparation within the specification [15].

6.5.2 Electrochemical corrosion tests in simulated seawater

It is uncommon for consumable manufacturers to attempt to provide information about application limits of their products. Yet this question is frequently asked by users. Ferric chloride corrosion testing is the most common corrosion tests to duplex grades. While they are good quality control tests they tell us nothing about service performance of the weld joint. But in the case of SDSS in seawater applications good estimates of the limits of use can be established from an understanding of chloride content and potential [46], [47]. This is because the CPT of welds and Critical Crevice Temperature (CCT) of flanged connections are strong functions of potential in chloride containing environments.

In natural seawater, stainless steels adopt a potential of about +350 mV SCE after a stable biofilm has formed. In offshore oil and gas seawater is used for cooling water and fire water purposes. In these instances, the seawater must be chlorinated to prevent marine fouling inside the pipes. The potential of stainless steels in chlorinated seawater (0.5 - 0.8 ppm chlorine typically) is +600 mV SCE.

In Sea Water Reverse Osmosis (SWRO) applications, seawater intake systems are chlorinated to avoid fouling but are then dechlorinated immediately prior to the high-pressure pumps that supply seawater to the membranes. The de chlorination process uses chemicals like Sodium Metabisulphite, that are oxygen scavengers by nature. This pulls the potential down to between +100 and +200 mV SCE. The potential is carefully controlled in this range to avoid damaging oxidation of the polyamide membranes. Both applications are important markets for these alloys.

Hence, it is possible to polarise welded samples to the potential of interest (i.e. for offshore oil and gas or SWRO situations) in simulated seawater solutions and steadily increase the temperature until the initiation of pitting or crevice corrosion is detected (as described in section 5.1.5b above) and establish the likely difference in performance between the grades in the different applications. Figure 19 shows the results of this test for welds made using both ZERON 100X(A) and ZERON 100X(B) consumables, and compared with those of the ZERON 100 base material.

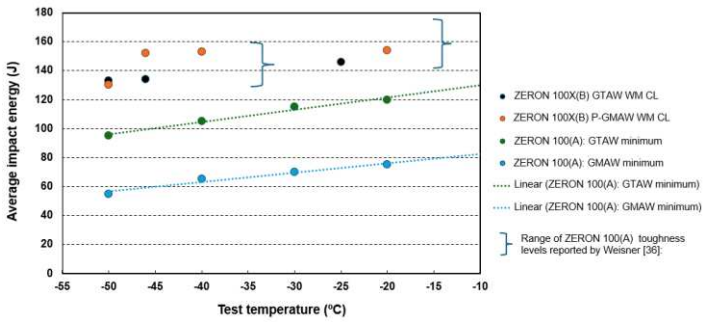


Figure 18. Charpy transition curves of ZERON 100X(B) GTAW and synergic P-GMAW weld metals

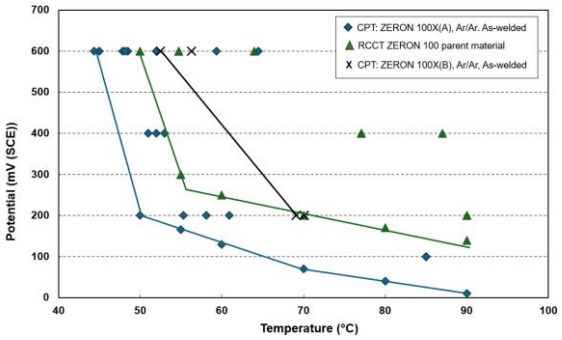


Figure 19. Effect of potential on RCCT of ZERON 100 parent material and CPT of ZERON 100 X(A) and ZERON 100X(B) GTAW Joints

Service experience is that pitting resistance of the SDSS welds is often the limiting case, whilst the crevice resistance of the parent material is somewhat higher. The lowest values measured for the CPT (of welds) and for the RCCT (of parent material, i.e. relative to the crevice former used in the test) are plotted against potential. The lower bound case is the CPT of welds made using ZERON 100X(A) composition consumables. At +600 mV SCE this is 44 °C. As the design condition for seawater cooling systems in the North Sea is typically 40 °C, this consumable provides about a 10% tolerance in temperature above the design case. However, experience has shown [46] that sometimes the design limit temperature is deliberately exceeded for operational reasons like dewaxing, or in error due to lack of control of chlorination levels or over heating by heater tracing wires used to prevent freezing. So, some tolerance to spikes in operating temperature is required. As the minimum CPT of ZERON 100X(B) welds is 52 °C, the use of this consumable provides considerable and important margins. Indeed, the CPT of these welds exceeds the RCCT of the parent material over the likely operating temperature range of the system.

The performances of ZERON 100X(A) welds made using pure Ar for both the shielding and backing gas and Ar+2.5%N_2 shielding gas with Ar backing gas, tested at +600 mV SCE have been reported elsewhere [27]. This work found that the while the average CPT was well differentiated at 53.9 °C and 63.9 °C respectively, the corresponding minimum CPT of these welds of 50.3 °C and 47.8 °C, was not. The minimum CPT of the ZERON 100X(A) deposit made using Ar+2.5%N_2 shielding gas was just below that measured for ZERON 100X(B) welded with Ar backing and shielding gas. So, the use of ZERON 100(B) welds negates the need for the used of more expensive Ar/N_2 shielding gas mixes.

In the case of SWRO applications, the maximum operating potential for the membranes is about +200 mV SCE. This corresponds with a CPT for ZERON 100X(A) weld of about 50 °C and ZERON 100X(B) of 69 °C. The seawater temperatures of regions like Middle East are typically about 35 °C

max. But there has been a tendency to co-locate SWRO plants with power stations and use the cooling water from the power station as the seawater feed for the RO plant. This has the benefit of using the power stations seawater intake system and having a local source of power for the plant. In the case of the Tampa Bay Water SWRO project in Florida, the design temperature for the cooling water exhaust from the Big Bend power station was 43°C and hence this became the design temperature for the seawater intake of the RO plant. In this case welds were made using ZERON 100X(A) consumables and the fabricated pipe spools were pickled by acid immersion in a nitric/hydrofluoric acid mix. This was done because it was found to increase the CPT in ferric chloride solution by 12 °C to 15 °C [48]. Hence, welding with Ar+2%N_2 shielding gas and acid pickling of fabricated pipe spools was considered the best practice for plants in the Middle East or those co-located with power stations. Subsequent electrochemical test [47] showed acid pickling gave a shift in CPT in simulated seawater at +200 mV from 50.3 ° C to 77.7 °C. The development of the optimised ZERON 100X(B) consumables now gives SWRO engineering contractors the opportunity to avoid acid pickling. This is particularly useful for closure joints that had to be flanged connections because welded joints could not be acid pickled.

To clarify, the CPT and CCT are stochastic in nature [49] [50]. Figure 9 shows some spikes in current density prior to the onset of stable pitting. These spikes are referred to as "metastable pitting" where pitting initiates, but the conditions are not severe enough to support stable pitting, so they re-passivate. Defects in the passive film like non-metallic inclusions, grain boundaries, deleterious phases, phases lean in Cr, Mo and N, other areas of segregation and heat tints [51] create a statistical population of weak points at which corrosion could initiate. So, stable pits arise from the probabilistic survival of metastable events rather than from a uniform material behaviour. This explains the scatter in results seen in Figure 19. Based on this, CPT and CCT at a particular potential should not be considered as the temperatures at which corrosion starts. It is best taken as the conditions under which the probability of at least one metastable pit surviving to stability on the tested surface becomes non-zero and large enough to be observed.

6.6 Weld radiographic quality

For a long period, super duplex stainless steel GMAW welding had been challenged by its susceptibility to weld porosity. In parallel to the ZERON 100X composition optimization, a separate project was executed by Lincoln Electric to develop a synergistic GMAW programme specifically for welding super duplex. The ZERON 100X(B) wire of both 1.0mm and 1.2 mm diameters were used as the filler wires for validation test of the new waveform. Cox and Acuna [52] reported that combination of the newly developed synergic P-GMAW waveform and the tri-mix shielding gas of 69.75%Ar+30%He+0.25%CO_2 optimized the droplet transfer and arc stability when using ZERON 100X(B) wire, thereby mitigated weld porosity. This finding was confirmed in the current work.

7 Overall summary

Table 23 details an overall summary of the test results of welds made using ZERON 100X(A) and ZERON 100X(B) type consumables against the technical requirements of some industry standards.

8 Conclusions

1) The design of ZERON 100X solid welding wire has been optimised to guarantee a minimum PREN of 42 with a typical heat analysis range of 43 to 44 together with modifications of additions of some other alloying elements. The full composition is kept within the AWS A5.9: ER2594 and ISO 14343-A: 25 9 4 N L classifications.
2) The filler metal is readily melted, rod rolled and drawn to wire of the required quality for the material in forms of welding consumables suitable for GTAW and GMAW processes.
3) Predictions of computational thermodynamics and empirical evaluations indicate a satisfactory phase balance of ferrite and austenite and expected precipitation characteristics of welds made using the optimised composition.

4) The tests of all-weld metal and weld joints in AWS assembly, small diameter thin-walled pipes and heavy thickness plates using the new wire have confirmed that;-
   - The metallurgical examination, corrosion and Charpy impact tests demonstrate a satisfactory the phase balance and the microstructure free from intermetallic phases.
   - The tensile properties at both ambient and elevated temperatures fully satisfy classification and industry standards.
   - Charpy impact toughness significantly exceeds the requirements of ISO 17781 Quality Level 1. Also, the absorbed impact energy levels attained using the synergic P-GMAW process with the 69.75%Ar+30%He+0.25%CO_2 tri-mix shielding gas is significantly higher than those obtained in the past using non-synergic processes with an Ar+He+2%CO_2 mixture.
   - The weld metal and HAZ hardness requirement of 350 HV max is readily achievable.
   - All-weld metal pass ASTM G48A and A932C at 40 °C with substantial safe margines. The ASTM G48A requirement of ISO 17781 is readily met up to a test temperature of 45 °C for welded joints.
   - The ASTM A932C requirement at 40 °C is readily met.
   - For GTAW welds, the CPT in chlorinated seawater, typical of oil and gas seawater cooling and fire protection systems is increased from a minimum of 44 °C for ZERON 100X(A) welds to a minimum of 52 °C for ZERON 100X(B) welds. The CPT in seawater typical of high-pressure seawater feed in SWRO plants is increased from 50°C minimum for ZERON 100X(A) welds to 68 °C minimum for ZERON 100X(B) welds.
5) The results indicate that the welds made with the new ZERON 100X(B) using Ar for both the shielding and backing gases can negate the need for an Ar+N_2 shielding gas to achieve satisfactory corrosion resistance, and similarly, they can render the acid pickling of fabricated pipe spools unnecessary in some applications.
6) The application of the newly developed synergic P-GMAW waveform and associated new gas mixture together with ZERON 100X(B) wire provides significantly more stable arc conditions and a substantially lower level of weld porosity than had been experienced in the past when conducting GMAW using a conventional process.

Table 23. A comparison of the results of ZERON 100X(A) and (B) welds vs. industry standards.

Property	Typical requirement	Specified min. (unless otherwise stated)	Typical for ZERON 100X(A) (PREN: 40min, 41 typical)	Optimized ZERON 100X(B) (PREN: 42min, 43-44 typical)
GMAW all-weld Rm	DNV-OS-F101	750 MPa	920 MPa	905 MPa
GMAW all-weld Rp0.2	DNV-OS-F101	550 MPa	725 MPa	715 MPa
Typical weld metal ferrite content (as-welded)	ISO 17781	50% ± 20%	50% ± 15%	50% ± 15%
Freedom from intermetallic phases	ISO 17781	Yes	Yes	Yes
Typical weld metal centre line impact energy at -46 °C	ISO 17781 (Quality Level 1)	50J avg. min. 40J min single values	130J avg. at -50°C (GTAW) 60J avg. at -50°C (GMAW)	133J avg. at -50°C (GTAW) 119J avg. at -50°C (GMAW)
Typical weld metal centre line hardness	DNV-OS-F101	350 max. HV10	290 max. HV10	330 max. HV10
Weld metal and welded joint corrosion property as per ASTM G48A	ISO 17781	≤4 g/m^2 weight loss and no pits at 35°C	≤ 4 g/m^2 weight loss and no pits at 35°C pass; Inconsistent results at 40°C	≤ 4 g/m2 weight loss and no pits at 45°C.
Weld metal and welded joint corrosion property as per ASTM A923C	Some oil and gas clients	≤10 mdd (approx. 1 g/m^2 weight loss) at 40 °C	Not generally achieved	Achieved
GMAW weld metal porosity	ASME IX	Synergic P-GMAW programme (such as the wave form recently developed by Lincoln Electric), in combination with a low CO_2 tri-mix gas of 69.75%Ar+30%He+0.25%CO_2 is necessary to achieve a stable arc and effectively suppress weld porosity meeting the industrial standard requirements. Without a synergic wave form and low levels of CO_2, arc instability prevails, resulting in unacceptable levels of weld metal porosity.		

Acknowledgements
The authors would like to acknowledge the support of Rolled Alloys, NeoNickel and Lincoln Electric for this work. C. Birch and B. Eden of BOC, A. Schlunt of Butting and P. Smallman of Valen Fittings for the provision of welders and welding services, C. Dascalu of Lincoln Electric Ductil SA for sample preparation and testing for all-weld metals, M. Jurgel and T. Kante of BGH for the provision of simulation software services, G. Warburton and R. Francis for useful discussions, AMS Testing, Exova and Element Materials Technology for provision of independent testing.

Author contributions:
Glenn Bynes: Methodology, phase simulation, experiment plan and execution, validation, results and data analysis, writing and editing of the manuscript.
Zhuyao Zhang: Methodology, phase simulation, experiment plan and execution, validation, results and data analysis, writing and editing of the manuscript.

Funding:
This research received no external funding.

Data availability:
The data that support the finding of this study will be available on reasonable request.

Declarations
Competing interests: The authors declare that they have no known competing financial interests or personal relationships that could have influenced the work reported in this paper.

Conflict of interests: On behalf of the authors, the corresponding author states that there is no conflict of interest. The authors have no competing interests to declare that are relevant to the content of this article

References
[1] Gonzales G.S., "Duplex and super duplex stainless steels in the oil and gas industry – characteristics for the correct application", Conf. Proc. of Offshore Technology Brazil. Paper No. OTC-36038-MS, Rio de Janeiro, Brazil, Oct. 2025.
[2] Lorenz K., Medawar G., "Uber das Korrosionsverhalten AustenitiScher Chrom-Nikel –(Molydan) Stahle mit und ohne Stickstoffzusatz unter Besonderer Berucksichtigung ihrer Beanspruchbarkeit in chlaridhaltigen Lodungen" (On the Corrosion Behaviour of Austenitic Chromium-Nickel (Molybdenum) Steels with and without Nitrogen Additions, with Particular Regard to their Performance in Chloride-Containing Solutions). ThyssenforSch.ung 1, 3 (1969), pp. 97-108.
[3] Trueman J.E., Coleman M.J. and Pirt K.R., "Note on the influence of nitrogen content on the resistance to pitting corrosion of stainless steels", British Corrosion Journal, Vol 12, Issue 4, Nov. 1977, pp. 236-238.
[4] Shone E.B., Malpas R.E. and Gallagher P., "Stainless steels as replacement materials for copper alloys in seawater handling systems", Trans. Inst. Marine Engineers, Vol.100, pp.193-206, 1988.
[5] Kovach K. and Redmond J.D., "Correlations between the CCT, PREN and long-term crevice corrosion data for stainless steels", Conf. Proc. of Corrosion'93, NACE, Paper 267, New Orleans, USA, Mar. 1993.
[6] Marshal A.W. and Farrar J.C.M., "The development of welding consumables for duplex stainless steels", Conf. Proc. of Duplex Stainless Steels'86. The Hague, Netherlands. 26-28 Oct. 1986. Paper 28. pp. 40-47.
[7] Fager S.A., "Design of consumables for the welding of super duplex stainless steel", Conference proceedings, Duplex Stainless Steels '91, Beaune, France, 28 – 30th Oct. 1991, pp. 403- 411.
[8] Holloway G.B., Zhang Z. and Gough P.C., "Corrosion testing of duplex and super-duplex weld metal", Conf. Proc. of Duplex Stainless Steel 2010, Beaune, France. 13-15 Oct. 2010.
[9] Jordan K.G. and Williams V.T., "Popeye project: hydraulic umbilical", Proc. of 28th Offshore Technology Conference, Paper No. OTC-8127-MS, Houston, USA, 6-9 May 1996.

[10] ASTM A240/A240M - 11: "Standard Specification for Chromium and Chromium-Nickel Stainless Steel Plate, Sheet, and Strip for Pressure Vessels and for General Applications", ASTM International, PA. USA, Mar. 2011.
[11] ASTM G48 - 11:" Standard Test Methods for Pitting and Crevice Corrosion Resistance of Stainless Steels and Related Alloys by Use of Ferric Chloride Solution", ASTM International, PA. USA, Sep. 2011.
[12] Olsen F.R., "Welding technology, 25% Cr super-duplex corrosion test challenges", http://www.nkfstavanger.org /Seminar2016/1-08-Olsen.pdf.eper x Corrosion Test Challe
[13] Colwell R.L. and Grocki J., "The validity of using ASTM A923 Test Method C on 25%Cr duplex stainless steels", Conf. Proc of NACE Corrosion 2017, Paper 8838, New Orleans, USA, 26-30 Mar. 2017.
[14] Raju A.," Challenges in qualifying welding procedures for super duplex steel S32760", Welding and Joining Matters, Issue 11, Apr. 2025.
[15] ASTM A923-22, "Standard Test Methods for Detecting Detrimental Intermetallic Phase in Duplex Austenitic/Ferritic Stainless Steels", ASTM International, PA, USA, 02 Jun. 2023.
[16] Woollin P. "Ferric chloride testing for weld procedure qualification of duplex stainless-steel weldments", Proc. of UK Corrosion and Eurocorr'94 Int. Conf., Bournemouth, UK, 31 Oct.-3 Nov.1994, Publ: London SW1Y 5DB, UK; The Institute of Materials; 1994. Vol.3. pp.51-60.
[17] Davidson R.M. and Redmond J.D., "Development of qualification tests for duplex stainless steel mill products", Conf. Proc. of NACE Corrosion 1991, Paper 302, Cincinnati, USA, Mar. 1991.
[18] Byrne G., "Issues in the testing of welds in super duplex stainless-steel grade UNS S32760". Welding and Joining Matters, Issue 13. Dec. 2025.
[19] Saunders N., Guo Z., Li X., Miodownk A.P. and Schille J.-Ph., "Using JMatPro to model material properties and behaviour", JOM: Journal of the Minerals, Metals & Materials Society, Vol 55, pp. 60-65, Dec. 2003.
[20] AWS Specification A5.9/A5.9M:2022 (ISO 14343:2017 MOD), "Specification for bare stainless welding electrodes and rods", American Welding Society, Sep. 2022.
[21] ISO 14343:2025, "Welding consumables - Wire electrodes, strip electrodes, wires and rods for arc welding of stainless and heat resisting steels – Classification", International Standards Organization, Jan. 2025.
[22] Kotecki D.J. and Siewert T., "WRC-1992 constitution diagram for stainless steel weld metals: a modification of the WRC-1988 diagram", The Welding Journal, Vol 71, No.5, pp. 171s-178s. May 1992.
[23] Lincoln Electric Company, Internal data summary.
[24] Hosseini V.A., Karlsson L., Engelberg D. and Wessman S., "Time-temperature-precipitation and property diagrams for super duplex stainless steel weld metals", Welding in the World, Volume 62, pp. 517-533, Jan. 2018.
[25] Nilsson J.O., "The physical metallurgy of duplex stainless steels", Conf. Proc. of Duplex Stainless Steel, Paper No. III.C.3, pp. 369-390, Beaune, France, 13-15 Oct. 2010.
[26] Leonard A.J., Woollin P. and Buxton D.C., "Effect of intermetallic phases on the corrosion resistance of super duplex and super austenitic stainless-steel weldments", Conf. Proc. of Stainless Steel World. The Hague, Netherlands, 13-15 Nov. 2001.
[27] Van Nassau L., Meelker H. and Hikes J., "Welding duplex and super-duplex stainless steels", Welding in the World, Vol 31, No.5, pp. 322-343, 1993.
[28] Zhang Z., van der Mee V., Golding M., Donate J. and Malioglou A., "Pitting corrosion resistance properties of super duplex stainless steel weld metals and influencing factors", Welding in the World, Volume 63, pp. 617-625, Dec. 2018.
[29] Byrne G., Sch..ulz Z., Warburton G. and Francis R., "Optimisation of the corrosion resistance of pipe butt welds in super duplex stainless steels", Conf. Proc. of European Federation of Corrosion, Paper 7805, 2024.
[30] Gunn R.N., "Duplex Stainless Steels – Microstructure, Properties and Applications", Abington Publishing, 1997.
[31] Metrode Products Limited Technical Document: "Welding Guidelines for Duplex & Super Duplex Stainless Steels", Issue 1, Feb. 2005.
[32] Oldfield J.W. and Sutton W.H., "Crevice corrosion of stainless steels: II. experimental studies", British Corrosion Journal, Vol 13, Issue 3, pp. 104-111, 1978.

[33] ASTM A995/A995M-20: "Standard Specification for Castings, Austenitic-Ferritic (Duplex) Stainless Steel, for Pressure-Containing Parts", ASTM International, PA, USA, 6 May 2020.
[34] Kotecki D.J., "Some pitfalls in the welding of duplex stainless steels", Stainless Steel World, pp. 51-57, Dec. 2009
[35] Gooch T.G. and Woollin P., "Metallurgical examination during weld procedure qualification for ferritic-austenitic stainless steels", Proc. of Stainless Steel World '99 Conference, Paper SSW99-021, pp. 729-738, The Hauge, The Netherlands, KCI Publishing BV, Nov. 1999.
[36] ISO 17781:2017, "Petroleum, Petrochemical and Natural Gas Industries — Test Methods for Quality Control of Microstructure of Ferritic/Austenitic (Duplex) Stainless Steels", International Standards Organization, Jul. 2017.
[37] Stevenson A.W., Gough P.G. and Farrar J.C.M., "The weldability of super duplex alloys – welding consumable procedure development for ZERON 100", International Institute of Welding Annual Assembly, The Hague, The Netherlands, Jul. 1991.
[38] Weisner C.S. "Toughness requirements for duplex stainless steels", Conf. Proc. of Duplex Stainless Steels'97, Paper D97 -107, pp. 979-990, The Netherlands, 21-23 Oct. 1997.
[39] Valiente Bermejo M.A., Karlsson L., Svensson L.E., Hurtig K., Rasmuson H., Frodigh M. and Bengtsson P., "Effect of shielding gas on welding performance and properties of duplex and super duplex stainless-steel welds", Welding in the World, Vol 59, No.2, pp. 239-249, Feb. 2014.
[40] NACE MR 0175 -2003 "Standard Material Requirements - Metals for Sulfide Stress Cracking and Stress Corrosion Cracking Resistance in Sour Oilfield Environments", Nace International Houston, Texas. 2003.
[41] ISO 15156:2003 "Standard Material Requirements - Metals for Sulfide Stress Cracking and Stress Corrosion Cracking Resistance in Sour Oilfield Environments Part 3: Cracking-resistant CRAs (corrosion-resistant alloys) and other alloys". International Standards Organisation, Geneva, Switzerland. Apr. 2003
[42] NORSOK M-601:2008 Edition 5, "A Welding and Inspection of Piping", Standards Norway, Lysaker, Norway, Apr. 2008
[43] NORSOK M630:2010 Edition 5, "Material Data Sheets and Element Data Sheets for Piping" Standards Norway, Lysaker, Norway, Sep. 2010.
[44] BS 4515-2:1999, "Specification for Welding of Steel Pipelines on Land and Offshore — Part 2: Duplex Stainless-Steel Pipelines", British Standards Institute, Apr. 1999
[45] DNV-OS-F101. "Submarine Pipeline Systems" Offshore Standard, Det Norske Veritas (DNV). October 2010.
[46] Byrne G., Sch..ulz Z., Sch..wartz A., Haman D., Warburton G.R. and Fajimi A., "The corrosion management of assets constructed in super duplex stainless steels topside and subsea – a supplier's perspective", Conf. Proc. of Corrosion 2016, Paper No. 6982, NACE International, 6-10 Mar. 2016.
[47] Byrne G., Francis R. and Wilson J., "Electrochemical potential and the corrosion resistance of stainless steels in SWRO applications", IDA International Desalination Conference, Dubai, UAE, Oct. 2009.
[48] Francis R. and Warburton G., "The effects of post weld surface treatments on the corrosion resistance of super duplex stainless steel welds in seawater", Conf. Proc. of Corrosion 2000, Paper 00630, NACE International, Mar. 2000.
[49] Laycock N. J., Moayed M.H. and Newman R.C., "Metastable pitting and the critical pitting temperature", Journal of the Electrochemical Society, Volume 145, No. 8, 1998.
[50] Laycock N. J. and Newman R.C., "Localised dissolution kinetics, salt films and pitting potentials", Corrosion Science, Volume 39, Issue 10-11, Oct-Nov 1997, pp. 1771-1790.
[51] European Commission: Directorate-General for Research and Innovation, Bylund, L.-Å. Et al "Guidelines for use of welded stainless steels in corrosive environments", Joinox Final Report Publications Office, 2018, https://data.europa.eu/doi/10.2777/980966.
[52] Cox C. and Acuna A., "Weld microstructure in duplex stainless steels using a novel waveform-gas combination", Duplex World Conference 2026, Rotterdam, the Netherlands, 6-7 May 2026.